Electrophoretic Injection within Microdevices

Maribel Vazquez,*,† Gareth McKinley,‡ Luba Mitnik,§ Samantha Desmarais,§ Paul Matsudaira,§ and Daniel Ehrlich§

New York Center for Biomedical Engineering, Department of Mechanical Engineering, The City College of the City University of New York, 140th Street and Convent Avenue T-250, New York, New York 10031, Massachusetts Institute of Technology, 77 Massachusetts Avenue, 3-250, Cambridge, Massachusetts 02144, and Whitehead Institute for Biomedical Research, 9 Cambridge Center, WI-339, Cambridge, Massachusetts 02142

The flexibility of the microfabricated format creates unique opportunities for study of the electrophoretic process. The present work utilizes digital images to capture the motion of DNA samples during pre-electrophoretic processes. A systematic study of DNA loading and strong sample stacking (sample concentration effects) was performed in order to analyze realistic DNA analysis conditions within microdevices. Using digital imaging and microscopy, DNA sample profiles within the injector were analyzed by deconvolving the geometrical intensity profile into different velocity groups. This analysis illustrates the evolution of molecular separation into distinct migrating populations within the injector itself. The present study performed DNA injections within microfabricated devices imposing run voltages between 85 and 850 V/cm. Data from 3 different offset lengths of a double-T cross-injector, 10 different applied voltages, and 2 different sample preparation protocols are presented.

Electrophoretic techniques are widely used for the separation of biological molecules and are becoming increasingly important in the era of proteomic analysis and biotechnology-derived drugs. Although electrophoresis is routinely performed in gels[1] and capillaries,[2,3] electrophoresis performed in microdevices has recently received particular attention because microfabrication[4−6] enables massively parallel analysis as well as total process integration.[6] The microfabricated channels dissipate heat effectively, such that separation voltages of up to 30 kV can be used to produce rapid, efficient separations in a short period of time. Such an effective combination suggests microdevices can be utilized for a variety of biotechnology applications. However, all potential applications of microdevices rely upon a complete understanding of device operation. To our benefit, although microfabricated channels have been used primarily to obtain measurements of DNA mobility via separations, they additionally provide a unique opportunity for direct visualization.

The present study visualizes the migration of fluorescently tagged DNA samples at the beginning of each separation, during electrophoretic injection. This stage of electrophoresis is particularly critical to separations because DNA molecules experience two distinct physical processes during their initial migration toward the anode, stacking[13−15] and destacking.[16] The dynamic process of sample stacking is distinct from the separation process and occurs within milliseconds of sample injection. It can be readily monitored and analyzed within the microdevice using the microscopy-based approach described here. The study of stacking is particularly important for electrophoretic separations because of the higher resolution data obtained from increased sample concentration. The primary goal of this research is to quantitatively describe the process of stacking and exploit its properties to achieve separations with higher resolution and read-lengths.

Microdevices. DNA separations are performed within microdevices using four different reservoirs (cathode, anode, sample, waste) and three distinct channel sections (separation channel, cross-injector, channel tail)[5] as seen in Figure 1. DNA molecules are loaded into microdevices using two steps. First, DNA is drawn into the microfabricated channel by a potential gradient that is imposed between the sample and waste reservoirs of the cross-injector. This process is called sample loading and is used to create a uniformly distributed DNA sample plug within the cross-injector offset. In the second step, termed electrophoretic injection, a run voltage is imposed between the cathode and anode of the

* To whom correspondence should be addressed. E-mail: vazquez@ccny.cuny.edu. Phone: (212) 650-5209. Fax: (212) 650−6727.

† The City College of the City University of New York.

‡ Massachusetts Institute of Technology.

§ Whitehead Institute for Biomedical Research.

(1) Stryer, L. *Biochemistry*, 3rd ed.; W. H. Freeman and Co.: New York, 1988.
(2) Pariat, Y. F.; Berka, J.; Heiger, D. N.; Schmitt, T.; Vilenchik, M.; Cohen, A. S., Foret, F.; Karger, B. L. *J. Chromatogr., A* **1993**, *652*, 57−66.
(3) Hebenbrock, K.; Williams, P. M.; Karger, B. L. *Electrophoresis* **1995**, *16*, 1429−1436.
(4) Schmalzing D.; Adourian A.; Koutny L.; Ziaugra L.; Matsudaira P.; Ehrlich D. *Anal. Chem.* **1998**, *70*, 2303−2310.
(5) Paegel, B. M.; Hutt, L. D.; Simipson, P. C.; Mathies, R. A. *Anal. Chem.* **2000**, *72*, 3030−3037.
(6) Lagally, E. T.; Mathies, R. A. *Anal. Chem.* **2001**, *73*, 565−570.
(7) Berka, J.; Pariat, Y. F.; Muller, O.; Hebenbrock, K.; Heiger, D. N.; Foret, F.; Karger, B. L. *Electrophoresis* **1995**, *16*, 377−388.
(8) Foret, F.; Szoko, E.l Karger, B. L. *Electrophoresis* **1993**, *14*, 417−428.
(9) Ruiz-Martinez, M. C.; Berka, J.; Belenkii, A.; Foret, F.; Miller, A. W.; Karger, B. L. *Anal. Chem.* **1993**, *20*, 2851−2852.
(10) Goetzinger, W.; Kotler, L.; Carrilho, E.; Ruiz-Martinez, M. C.; Salas-Solano, O.; Karger, B. L. *Electrophoresis* **1998**, *19*, 242−248.
(11) Viovy, J. L. *Rev. Mod. Phys.* **2000**, *72*, 813−872.
(12) Sassi, A. P.; Barron, A.; AlonsoAmigo, M. G.; Hion, D. Y.; Soane, D. S.; Hooper, H. H. *Electrophoresis* **1996**, *17*, 1460−1469.
(13) Palmer, J.; Munro, N. J.; Landers, J. P. *Anal. Chem.* **1999**, *71*, 1679−1687.
(14) Morales, S.; Cela, R. *J. Chromatogr., A* **1999**, *846*, 401−411.
(15) Guttman, A. *Anal. Chem.* **1999**, *71*, 3598−3602.
(16) Gebauer, P.; Thormann, W.; Bocek, P. *Electrophoresis* **1995**, *21*, 11−19.

10.1021/ac0110045 CCC: $22.00
Published on Web 00/00/0000

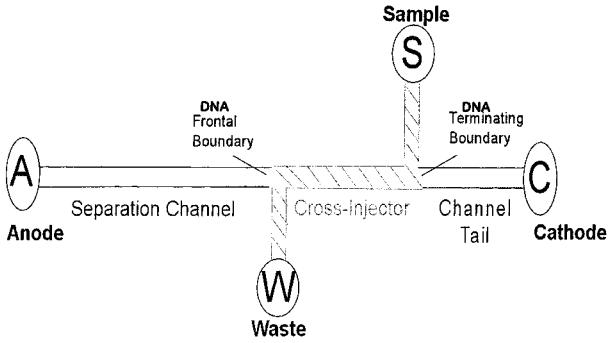

Figure 1. Schematic of a conventional microdevice illustrating an 11-cm-long separation channel, a "double-T" cross-injector configuration, and a minimal channel tail section. The sample channel is depicted on the upper-right-hand side of the image, and the waste channel is shown on the lower left-hand side. The frontal and terminating boundaries of the DNA sample are also identified.

microdevice in order to initiate DNA migration toward the anode. During the early stages of injection, DNA molecules migrate rapidly within the sample plug of the cross-injector but experience an abrupt drop in velocity upon reaching the lower field within the high-conductivity electrolyte buffer.[20,21] The subsequent decrease in velocity creates a thin and focused zone of DNA molecules at the interface between the sample and separation buffer, called the stacked plug[16] or stacked sample.[19]

To visualize the motion of DNA samples during electrophoretic injection, DNA molecules were fluorescently tagged with propidium iodide and observed using an epifluorescence microscope. Once the sample was introduced into the microdevice, detailed images of the sample loading within the cross-injector and subsequent electrophoretic injection into the separation channel were captured using a CCD camera. These images demonstrate the complete process of sample loading and stacking, as well as illustrate the effect of many commonly used protocols. We quantitatively measured the width of the stacked sample using the values of intensity recorded for each pixel within the digital images. Experimental data gathered from the images are used to identify specific parameters that define stacking and its level of intensity. Additionally, we developed a model that represents the sample plug by *N* Gaussian distributions of DNA molecules that migrate with similar group velocity throughout injection. The transient redistribution of DNA molecules within each Gaussian then describes the formation and propagation of the stacked sample during injection. The results are used in conjunction with an analytical model[16,23] to build an empirical tool that gauges the level of stacking experienced by DNA molecules under various experimental conditions.

Finally, results from video microscopy are correlated with electropherograms in order to quantify the benefits of increased stacking to DNA sequencing. A new high-voltage injection protocol is introduced in order to examine the effects of increased stacking on DNA read lengths and resolution. This study performed DNA injections within microdevices imposing run voltages of 85−850 V/cm between the cathode and anode ports of a microfabricated device, depicted in Figure 1. Data from 3 different offset lengths of a double-T cross-injector, 10 different applied voltages, and 2 different sample preparation protocols are presented.

THEORY

Mechanism of Stacking. The phenomenon of stacking within a cross-injector operates on the same principle as stacking in a capillary.[18−20,22] When an electric field is applied along a channel, the flux of ions within the channel generates a current that is described by its current density, *I*.[24] This vector points in the direction of current flow and is strongly influenced by the ionic conductivity of the medium.

$$I = -\kappa\nabla(\Phi) \qquad (1)$$

In the above expression, κ denotes the ionic conductivity of a material, expressed in Siemens per centimeter (S/cm), while $\nabla\Phi$ represents the potential gradient, or electric field applied along the material (in units of V/cm). Due to the chemical composition required for separations, the ionic conductivity of the buffer electrolyte solution, κ_B, is typically much higher than that of the DNA solution, κ_D. Hence, when the run voltage is applied along the channel, a disproportionate amount of the potential drop is found along the low-conductivity-sample plug.[28] However, as the DNA molecules migrate toward the buffer solution, they exhibit an abrupt drop in velocity upon experiencing the lower potential gradients present within the electrolyte. The sudden decrease in velocity creates a very thin and concentrated zone of DNA molecules at the injector exit via the mechanism called "stacking".[8,16,18,19]

Moving Boundary Equation. Stacking can be described analytically using the one-dimensional moving boundary equation first described by Longsworth.[25] Since DNA molecules are constrained within the cross-injector prior to separation, the sample plug has two DNA boundaries, the frontal and terminating boundaries. The frontal boundary is formed between the sample plug and buffer region closest to the anode, and the terminating boundary is formed between the sample plug and buffer closest to the cathode. Molecules on the frontal boundary immediately migrate out of the sample plug and into the buffer electrolyte during injection because of their proximity to the anode.[16,23] In contrast, molecules on the terminating boundary migrate toward the anode within the sample plug at all times during injection as a consequence of their position within the cross-injector. Using the moving boundary equation, stacking is described by utilizing a Lagrangian reference frame that migrates concurrently with the sample's frontal interface. The stacking velocity can be determined

(17) Wu, Y. C.; Berezansky, P. A. *J. Res. Natl. Inst. Stand. Technol.* **1995**, *100*, 521−527.
(18) Zhang, C. X.; Thormann, W. *Anal. Chem.* **1996**, *68*, 2523−2532.
(19) Beckers, J. L.; Bocek, P. *Electrophoresis* **2000**, *21*, 2747−2767.
(20) Quirino, J. P.; Terabe, S. *J. Chromatogr., A* **1999**, *850*, 339−344.
(21) Guirino, J. P.; Terabe, S. *Electrophoresis* **2000**, *21*, 355−359.
(22) Shultz-Lockyear L. L.; Colyer, C.; Fan, Z. H.; Roy, K. I.; Harrison, D. J. *Electrophoresis* **1999**, *20*, 529−538.
(23) Russel, W. B.; Saville, D. A.; Schowalter, W. R. *Colloidal Dispersions*, 2nd ed.; Cambridge University Press: New York, 1990.
(24) Halliday, D.; Resnick, R. *Fundamentals of Physics*, 3rd ed.; John Wiley & Sons: New York, 1980.
(25) Longsworth, L. G. *J. Phys.* **1943**, *61*, 1755−1765.
(26) Probstein, R. F. *PhysicoChemical Hydrodynamics*, 2nd ed.; John Wiley & Sons: New York, 1994.
(27) Deleted in proof.
(28) Grossman, P. D.; Colburn, J. C. *Capillary Electrophoresis, Theory and Practice*; Academic Press: San Diego, CA, 1992.

from the expression[16,25]

$$\frac{\mu C_{D,S}}{\kappa_S} - \frac{\mu C_{D,B}}{\kappa_B} = \frac{V_{ST}(C_{D,S} - C_{D,B})}{I} \quad (2)$$

where μ represents the electrophoretic mobility of DNA, $C_{D,S}$ is the concentration of DNA, D, present in the sample plug, S, and $C_{D,B}$ is the concentration of DNA in the electrolyte buffer, B. The ionic conductivity of the sample plug, S, is denoted by κ_S, and κ_B represents the ionic conductivity of the buffer, B. The parameter V_{ST} represents the stacking velocity, i.e., the velocity of the terminating boundary with respect to the frontal boundary, and I is the total current density within the channel. The current density is defined by the total flux of ions within the channel, which in the general case can be attributed to electromigration, diffusion, and convection as expressed in eq 3, where Φ is the electric

$$I = -\kappa\nabla\Phi - F\sum z_i D_i \nabla C_i + Fu\sum z_i C_i \quad (3)$$

potential (in V), F is Faraday's constant of value 9.65×10^4 C/mol, κ is ionic conductivity (in S/cm), D is diffusivity (measured in cm^2/s), z is the dimensionless valence number of the ith ion, u is the bulk velocity (which is identically zero for a fixed sieving matrix), and C is concentration in ($1/m^3$). For the general problem, the conductivity can change in time due to redistributions of ions within the channel. As shown previously,[24,26] an expression for the stacking velocity, V_{ST}, can be obtained utilizing eqs 2 and 3 simultaneously.

Potential Gradients. Stacking has been predominantly studied by assuming the potential gradients within the sample plug remain constant throughout the process.[28−30] One of the more complete stacking models proposed by Gebauer et al.[16] defined two types of stacking termed frontal- or terminator-type stacking. DNA exhibits frontal-type stacking when molecules accumulate near the frontal boundary of the sample plug, nearest the anode. Conversely, DNA exhibits terminator-style stacking when molecules accumulate near the terminating boundary of the sample plug, nearest the cathode. In the first type of stacking, molecules are concentrated on the frontal boundary. To first order, with constant potential gradients within the sample plug, DNA molecules experience an abrupt decrease in velocity only when they reach the frontal boundary. Here, molecules are influenced by the lower potential gradients of the electrolyte buffer almost immediately and concentrate on the frontal boundary of the sample. In terminator-type stacking, molecules are concentrated on the terminating boundary of the sample. Here, the potential within the sample plug is continuously modified as the sample width diminishes, imposing the largest gradients near the terminating boundary[16] and the smallest potential gradients toward the frontal boundary. Accordingly, molecules accelerate during electrophoretic injection when the stacked sample reaches their position. A concentrated, stacked plug of DNA molecules is developed on the sample's terminating boundary as a larger number of molecules are accelerated by the high potential gradient associated with this interface.

(29) Mosher, R. A.; Saville, D. A.; Thormann, W. *The Dynamics of Electrophoresis*; VCH Publishers: London, 1988.

MATERIALS AND METHODS

Sample loading and electrophoretic injections of DNA solutions were observed within the cross-injector portion of microdevices using an inverted, epifluorescence microscope (Nikkon TE-3000). Microfabricated devices used in this study utilized a double-T cross-injector configuration, identical cross-sectional areas, and equal separation lengths. The inner walls of the microfabricated channels were coated using a Hjerten procedure[32] while a polymeric sieving solution was loaded into the channel center at rates that ensured minimum degradation.[33] Channels were reloaded with a new volume of sieving solution prior to, and between, successive sample loadings and injections. Additionally, preelectrophoresis was performed at 300 V/cm for 3 min, before each sample loading.

DNA Samples. Both monodisperse and polydisperse solutions of DNA were utilized for the study of electrophoretic injection. Monodisperse solutions were prepared using 10^{-10} M concentrations of single-stranded, 500-base-long molecules obtained through PCR amplification of the M13mp18 vector (New England Biolabs, Beverly, MA). Polydisperse reactions were prepared using 10^{-10} M concentrations of DNA sequencing reactions obtained from the M13mp18 vector. Sequencing reactions were composed of single-stranded DNA molecules ranging from 1 to 7300 bases in length, including the template molecule.[34] Polydisperse samples were synthesized via standard cycle sequencing chemistry with AmpliTaq-FS, Big Dye Terminator labeling (Applied Bio-systems/Perkin-Elmer Corp., Foster City, CA). A total of 200 μg of template DNA was used per 96-sample preparation. Cycle sequencing was performed on a Genius Thermocycler (Techne, Duxford, Cambridge, U.K.) consisting of 15 cycles of 10 s at 95 °C, 5 s at 50 °C, and 1 min at 70 °C, followed by 15 cycles of 10 s at 95 °C and 1 min at 70 °C. All samples were desalted using Centri-Sep spin columns (Princeton Separations, Adelphia, NJ). The spin columns were hydrated for at least 30 min by adding 800 mL of deionized water. The interstitial volume was excluded by spinning the columns for 3 min at 3000 rpm. The sequencing sample was diluted in 40 μL of deionized water and then placed in the column and spun for 3 min at 3000 rpm. The resulting sample volume was diluted to 50 μL with deionized water, and a 10-μL aliquot was then pipetted onto the electrophoretic device during experiments. Samples were also fluorescently labeled with 10^{-10} M propidium iodide so that their fluorescent signal emitted under illumination could be recorded by a CCD camera.

Micromachining. Electrophoretic microdevices were made from 150-mm-diameter glass wafers (Corning, NY) using techniques described in the literature.[4] The devices each utilize a double-T cross-injector geometry for sample loading, which consists of a sample, offset, and waste channel. The separation channel is hemispherical in cross section, approximately 40 μm deep and 90 μm wide, with an effective length of 11.5 cm. The sample and waste channels of each cross-injector are ~5.0 mm in length and horizontally offset by a distance of 150, 250, or 500 μm. Glass reservoirs (Ace Glass, Vineland, NJ) of 50-μL volume

(30) Palusinksi, O. A.; Graham, A.; Mosher, R. A.; Bier, M.; Saville, D. A. *AIChE J.* **1986**, *32*, 205−223.
(31) Deleted in proof.
(32) Hjerten, S. *J. Chromatogr.* **1985**, *347*, 191−198.
(33) Vazquez, M.; Schmalzing, D.; Matsudaira, P.; Ehrlich, D.; McKinley, G. *Anal. Chem.* **2001**, *73*, 3035−3044.

are affixed around the laser-drilled holes that access the electrophoretic channel in order to contain the appropriate volumes of sample and buffer solutions.

Electrophoresis. DNA sequencing reactions were loaded into the cross-injector by applying a negative potential of 2300 V (corresponding to 150 V/cm) to the sample reservoir and keeping the waste reservoir at ground. During sample loading, the buffers in both the anode and cathode reservoirs were left floating. Leakage of excess sample from the cross-injector into the separation channel was prevented with a small electric pull-back voltage (~40 V/cm) applied to both halves of the loading channel 10 s after injection. In all experiments, a run voltage between 85 and 850 V/cm was applied for 5 s during electrophoretic injection and then reduced to the standard 150 V/cm for full separation using a voltage relay switch.

To obtain resolution data from electropherogram analysis, the G-traces of Big Dye Terminator-labeled DNA sequencing reactions were used.[4] The G-traces were selected due to minimal cross-talk and ease of tracking isolated peaks over the entire range of fragment sizes. From the resulting electropherograms, the migration times of the sequencing fragments were plotted against their base number and fitted with a Gaussian distribution using Microcal Origin 6.0 software (Microcal Software Inc., Northampton, MA).

Microscopy and Digital Imaging. Electrophoretic injections were observed using the 10× objective of an inverted, epifluorescence microscope (Nikkon TE-3000). The microscope is equipped with filter cubes (Nikkon 34-TA47), CCD camera (Orca-Hamamatsu 54327), and a mercury lamp for the illumination of samples. The CCD camera collected the intensity of the fluorescent signals emitted by the labeled molecules at a rate of 8 frames/s using a simple time-lapse protocol (Openlab software). These data was then converted into 8-bit digital images with a 256 gray-level scale. Using this scale, an intensity value of 1 is recorded when the camera detects a very low amount of fluorescence emitted by the labeled molecules. Since the molecules are uniformly tagged with propidium iodide, an intensity value of 1 also corresponds to a low number of molecules in the pixel of interest. On the other extreme, an intensity reading of 256 indicates the camera is near its saturation limit, meaning the strength of the fluorescent signal emitted by the molecules is approaching the camera's recordable limit. To utilize the full dynamic range of the camera, low concentrations of propidium iodide were used to ensure intensity values were maintained between 30 and 200 on the gray scale at all times.

The microscopy images shown are all two-dimensional projections of a three-dimensional channel. Note that although the depth of the channel is not visible in the images, this third dimension influences the intensity of the fluorescent signal recorded by the CCD for each pixel. That is, a labeled molecule positioned farther away from the microscope objective may exhibit a lower fluorescent intensity than if it were located at a closer distance. This is a particular problem when the intensity of pixels within a channel fabricated with uneven depth is being measured. Since the channels used for this research were hemispherical, not rectangular, pixels closer to the channel walls have different depths than those located in the center. Hence, to eliminate any three-dimensional effects in the digital image, no matter how slight, only pixels in the centerline of the channel were used to describe the shape of the sample plug during stacking. The intensity of each pixel is plotted against its position within the cross-injector in order to build a mathematical profile of the shape of the DNA sample plug. This method is applied to the images gathered from the electrophoretic injections of both monodisperse and polydisperse samples.

RESULTS

In this section, the qualitative observations and quantitative conclusions derived from the video microscopy of electrophoretic injection are discussed. The data gathered via digital imaging illustrate the complex stacking behavior exhibited by DNA samples during electrophoresis.

Electrophoretic Injection. Although DNA molecules are introduced into microdevices via sample loading, molecules do not migrate toward the separation channel until after electrophoretic injection is initiated. As mentioned in the introduction, after a 3-min sample-loading protocol, the load voltage along the cross-injector is turned off, and a run voltage between the cathode and anode is applied. The subsequent electrophoretic injection of both mono- and polydisperse samples are shown in Figure 2. The injection of the monodisperse sample is represented by six digital images, shown on the left-hand side of the figure, and the injection of the polydisperse sample is represented by the images seen on the right-hand side. Both injections were initiated by a run voltage of 150 V/cm and utilized a small pull-back voltage[8] of 40 V/cm imposed along the cross-injector. The sample injection began when the run voltage was applied at time $t = 0$ s and ended when the sample plug exited the cross-injector at $t = 3$ s.

At time $t = 0$ s, DNA molecules of the monodisperse sample are uniformly distributed within the offset of the cross-injector, as a consequence of sample-loading protocols. As the electrophoretic injection is initiated, the width of the sample plug is visibly diminished as molecules migrate toward the anode. During this migration, the sample's terminating boundary becomes increasingly bright, as first seen at $t = 1.8$ s, indicating the formation of an increasingly concentrated plug of DNA molecules. The high color density seen near the sample's terminating boundary qualitatively illustrates the development of the stacked sample and its progression toward the separation channel. At time $t = 3.0$ s, the redistribution of DNA molecules is complete, as the sample plug is reduced to a very concentrated stack near the exit of the cross-injector.

In contrast, the electrophoretic injection of the polydisperse sample under identical conditions is shown on the right-hand side of Figure 2. The sample contains 10^{-10} M DNA sequencing reactions, purified via spin columns as discussed in the Materials and Methods section. At $t = 0$ s, the polydisperse solution is also uniformly distributed within the injector offset as a consequence of sample loading. However, as molecules migrate toward the anode, the formation of the stacked sample at the rear of the plug is rather distinct. Whereas molecules of the monodisperse sample formed a tightly concentrated stacked sample at the terminating boundary of the plug, the stacked sample developed by the polydisperse molecules is nonuniform and positioned toward the center of the sample plug. As seen at time $t = 2.4$ s, while molecules from the monodisperse sample exhibit a sharp terminating boundary, the terminating boundary of the polydisperse

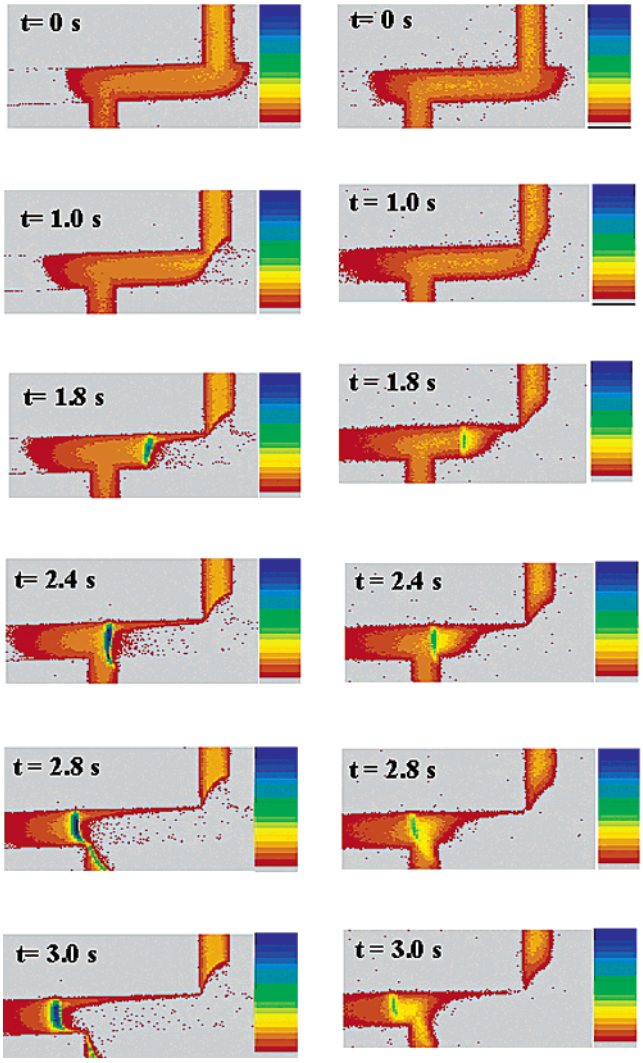

Figure 2. Set of six digital images on the left-hand side of the figure illustrating the experimentally observed electrophoretic injection of the 10^{-10} M monodisperse DNA solution. The opposite set of images on the right-hand side of the figure depicts the electrophoretic injection of the 10^{-10} M DNA sequencing reaction purified using spin columns. Injections were initiated by a 150 V/cm run voltage following a 3-min sample loading performed at 300 V/cm. The run voltage was first applied at $t = 0$s.

sample plug remains diffuse during injection. Further, molecules of the polydisperse sample develop a fully stacked sample plug more slowly than do the molecules of the monodisperse sample, as evidenced by their respective stack locations at time $t = 3.0$ s.

The digital images in Figure 2 illustrate terminator-type stacking during both injections because the stacked sample is initiated on the terminating boundary of each sample plug. As discussed in the Potential Gradients section, the stacked sample develops on the terminating boundary of the sample plug due to the changing potential gradients within the sample. The largest gradients are located near the terminating boundary and accelerate molecules ahead of it to develop a stacked sample at the terminating boundary of the sample plug. Note, if this system exhibited frontal-type stacking, a concentrated DNA stack would have been formed on the sample's frontal boundary and the images of Figure 2 would have illustrated brighter regions near the frontal boundary.

Pull-Back Protocols. One observation made from Figure 2 is the effect of the pull-back voltage on electrophoretic injections. A pull-back voltage, V_{PB}, is a small, negative potential gradient applied between the sample and waste reservoirs of the cross-injector in order to prevent DNA leakage into the separation channel.[4] Pull-back voltages were applied simultaneously with injection during both experiments in order to simulate the commonly used protocol. The applied pull-back voltage extracted roughly 10% of DNA molecules within the monodisperse sample, and 15% of molecules within the polydisperse sample, as determined by signal intensity measurements of Figure 2. The pull-back voltage appears particularly harmful to the injection of the polydisperse sample because it preferentially removes molecules from the stacked sample and affects the redistribution of DNA molecules behind the stacked sample. As seen in Figure 2, the sample's terminating boundary is visibly "tilted" upon migrating through the pull-back field of the cross-injector. Subsequent experiments indicate that DNA molecules within the channels of the cross-injector do not leak into the separation channel if V_{PB} is not applied immediately. Hence, a pull-back voltage initiated 5−10 s after injection enables the complete migration of the sample plug into the separation channel without molecular loss or leakage from injector channels. The benefit of this delay has been experimentally verified for running voltages between and 850 V/cm.

Intensity Profiles. The images in Figure 2 illustrate that differences in mobility within the mono- and polydisperse samples are significant even during the stacking process. The images also provide excellent visual representations of terminator-type stacking. In this section, we use the microscopy data quantitatively by measuring the intensity of pixels in each image. Intensity measurements of pixels located along the channel centerline in each image are plotted against their position in the channel, x, and time, t. We refer to these intensity graphs as DNA profiles and utilize them to represent the changing molecular distribution of the sample throughout its electrophoretic injection.

Intensity profiles of the electrophoretic injection of the monodisperse and polydisperse samples are represented by the heaviest lines in Figure 3. Each injection is represented by five plots, illustrating the distribution of DNA molecules within the sample at the specified time indices. The initial shape of each sample plug at $t = 0$ s is rectangular, consistent with the uniform distribution obtained via sample loading. As the electrophoretic injection progresses, however, the formation of the stacked sample is illustrated by a peak that grows in intensity near the terminating boundary of the sample. Its continuous growth represents the increasing number of molecules that begin to migrate within the concentrated stacked sample. The profiles of both samples indicate there are populations of DNA molecules whose velocities vary with time throughout injection. This is expected, as changes in the ion distribution within the injector cause time-varying changes in the potential gradients which act upon different populations of DNA at different times. As a result, DNA molecules experience different velocities at different locations within the sample plug.

***N* Gaussian Model.** As seen in Figures 2 and 3, the redistribution of polydisperse and monodisperse samples is not the same. Molecules of the monodisperse sample, shown on the left-hand side of both figures, exhibit a profile that appears Gaussian by the end of injection. The stacked monodisperse

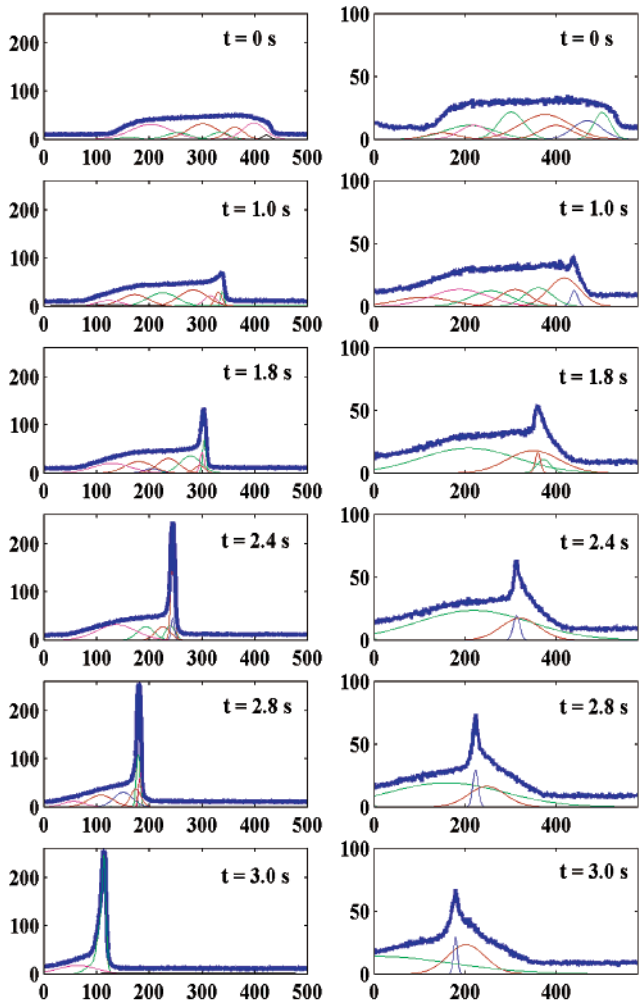

Figure 3. Set of six graphs on the left-hand and right-hand sides of the figure illustrating the intensity measurements taken during the electrophoretic injection at 150 V/cm of the 10^{-10} M monodisperse DNA sample and 10^{-10} M polydisperse DNA sample, respectively. The heaviest lines, shown in blue, represent measurements of intensity obtained from pixels located along the centerline of the channel at the indicated time. The lighter sets of lines within each graph illustrate the *N* Gaussian model representation applied to each sample. The sample plug was initially divided into 10 Gaussians at time $t = 0$ s and numerically decomposed into the minimum number of Gaussians needed to describe the various regions of electrophoretic velocity during injection. As seen, the velocity of DNA molecules from the monodisperse sample is largely described by one predominant Gaussian toward the end of the injection, and the molecular velocities of the polydisperse sample are described by three Gaussians shortly after injection is initiated.

sample is much more concentrated than that of the polydisperse sample seen on the left-hand side of each figure. Although the polydisperse sample also displays a peak in its distribution during injection, a large percentage of molecules ahead of that peak remain unstacked by the end of injection.

To quantitatively describe the redistribution of DNA molecules during electrophoretic injection, we take a finite element approach and divide the initial sample plug, at time $t = 0$ s, into N velocity domains illustrated by the lighter lines in Figure 3. Gaussians are labeled 1 through N, where the first Gaussian represents molecules that exhibit the slowest velocity, V_1, and the Nth Gaussian describes the distribution of molecules that migrate with the fastest velocity, V_N. Consequently, the first Gaussian is located closest to the frontal boundary of the sample while the Nth Gaussian is positioned nearest the sample's terminating boundary.

As the sample width decreases during injection, the potential gradients within the sample plug change similarly. Since the samples illustrate terminator-type stacking in Figures 2 and 3, the larger potential gradients of the sample plug are presumed to be at the terminating boundary. Initially, at time $t = 0$ s, the potential gradient is highest near the terminating boundary of the sample and decreases toward the frontal boundary. At some time $t = t_N$, the width of the sample plug is diminished, and the distribution of potential gradients within the sample is no longer identical to those observed at $t = 0$ s.

In our model, as the terminating boundary approaches the frontal boundary during injection, the higher potential gradients associated with the stacked portion of the sample incrementally increase the velocity of molecules in its path. Since DNA accelerates incrementally under the approaching higher potential gradients, the population of DNA molecules within each Gaussian changes rapidly with time and position. That is, a molecule initially within the population of the $(N - 1)$th Gaussian, traveling with velocity $V_{(N-1)}$, is accelerated by the higher potential gradients approaching its position. This molecule then obtains a new, higher velocity, V_N, and transfers to the population of the faster moving Nth Gaussian. Similarly, as the higher potential gradients approach the molecules within the $(N - 2)$th Gaussian, these molecules are accelerated to a higher velocity group $V_{(N-1)}$. These molecules then quickly exit the slower $(N - 2)$th Gaussian and transfer within the adjacent $(N - 1)$th Gaussian. In this manner, molecules transfer within sequentially labeled Gaussians several times during injection. Consequently, populations of fast moving Gaussians steadily increase during the formation of the stacked sample while populations of slower Gaussians diminish to zero. Intermediate Gaussians, denoted 1 through $(N - 1)$, therefore, represent regions of transient DNA velocity. Note, however, that all Gaussians are needed during the formation of the stacked sample to more accurately describe the redistribution of DNA molecules based upon their velocity.

***N* Gaussians of the Monodisperse and Polydisperse Samples.** The model is now used more specifically to describe the electrophoretic injection of the mono- and polydisperse samples, respectively. Importing the data obtained from the intensity profiles into Matlab, the molecular distribution of the sample plug at each time step is decomposed into 10 Gaussian velocity groups as shown on the left-hand side of Figure 3. The first Gaussian represents the motion of DNA molecules nearest the frontal boundary of the sample while the tenth Gaussian represents those molecules nearest the sample's terminating boundary. Using Matlab, a mathematical fit is made to the area of the sample plug with minimum error. At time $t = 1.8$ s, an increasing number of molecules are accumulated within the tenth Gaussian as its intensity increases rapidly. Similarly, the amplitude and location of all intermediate Gaussians change rapidly as a larger number of molecules are transferred toward the tenth Gaussian. During this time, the number of Gaussians needed to describe the different velocities of the sample is reduced, as seen by the Gaussian decomposition shown at time $t = 2.4$ s. Molecules of intermediate Gaussians continue to transfer rapidly within

adjacent populations until they migrate with an increased velocity, V_N, and accumulate within the population of the tenth Gaussian. As additional molecules continue to transfer toward the tenth Gaussian, the final stacked sample plug seen at time $t = 3.0$ s is represented by one large Gaussian at the sample's terminating boundary and one rather small Gaussian near the frontal boundary.

The model similarly describes the formation of the stacked sample using polydisperse molecules. Using the N Gaussian model, the stacking of the sample plug is again described by the migration of 10 Gaussian velocity groups positioned between the frontal and terminating boundaries as described earlier. Just as before, molecules able to accelerate to the fastest group velocity, V_N, transfer into the population of the Nth Gaussian. However, in this case, the numerous molecular lengths increase the complexity of DNA redistribution during injection because molecules also separate according to their different molecular weights. As seen on the right-hand side of Figure 3, molecules from the sequencing reaction quickly transfer within $N = 10$ Gaussians to a reduced number of Gaussians almost immediately. By $t = 2.0$ s, the remaining dynamics of the injection are well described by a minimum of three strong Gaussians. Unlike the monodisperse sample seen on the left-hand side of Figure 3, molecules of the polydisperse sample do not largely accumulate into a single, final velocity group. These data must now be used to explain the emergence of specifically three velocity domains.

Correlation with DNA Sequencing Results. The results taken at the injector exit are now correlated to the more traditional electrophoretic data measured at the end of the separation channel, namely, electropherograms. A typical electropherogram for a sequencing solution labeled with Big Dye Terminators displays a series of small, individual peaks followed by large peak at the end of the experiment. Each peak represents the fluorescence intensity emitted by a particular population of DNA molecules with the same molecular weight. The large peak seen at the end of the electropherogram represents the failure of molecular sieving for large molecules, usually attributed to a slow rate of reptation. By plotting the electrophoretic mobility, μ (obtained from electropherograms) against DNA size, N, on a log−log scale, three velocity domains emerge to describe the migration of small-, medium-, and larger-sized molecules. The mobility of the smallest molecules within the sequencing reaction demonstrates a negative dependence on size, while that of the next set of molecules is inversely proportional to size. The mobility of the largest molecules is altogether independent of size. The simplest assignment for this distribution corresponds to the classical modes of migration via molecular sieving[35,36] reptation without orientation,[37,38] and reptation with orientation,[39,40] respectively. Performing the size-based analysis previously described by Heller[40] under near-identical conditions, DNA molecules less than 150 bases in length migrate via molecular sieving while molecules greater than 800 bases migrate via biased reptation. The remaining molecules, 150−800 bases in length, migrate via reptation. Hence, we conclude that each Gaussian distribution defined by our model corresponds, approximately, to a particular velocity domain seen in the electropherogram. That is, the fastest Gaussian in the injector represents the migration of the smallest molecules, which transport via molecular sieving. The intermediate Gaussian represents the reptative migration of longer molecules, and the slowest Gaussian illustrates the motion of the longest molecular fragments via reptation with orientation.

Table 1. Measurements of Velocity for DNA Molecules of Various Sizes Obtained from the Electrophoretic Injection of 10^{-10} M Polydisperse Samples within 250-μm-Long Injector Offsets [a]

DNA (bases)	V_A (cm/s)	V_E (cm/s)	V_{NGM} (cm/s)
	Spin-Column-Purified Samples		
30	0.032	0.029	0.030
182	0.028	0.027	0.026
300	0.026	0.026	0.025
517	0.024	0.023	0.025
800	0.0095	0.0089	
	Ethanol-Precipitated Samples		
30	0.034	0.029	0.033
182	0.029	0.026	0.025
300	0.027	0.025	0.024
517	0.025	0.023	0.021
800	0.0091	0.0084	0.0081

[a] The parameter V_A denotes velocities obtained analytically, the symbol V_E represents those velocities measured experimentally from electrophoregrams, and the parameter V_{NGM} illustrates the velocities measured using the N Gaussian model representation of the sample plug.

Two different types of comparisons are performed in order to support this particular assignment: molecular weight versus Gaussian velocity and sample composition versus Gaussian area. First, the velocity of each Gaussian is obtained by plotting the position of its mean as a function of time. The velocities calculated via the slope are then compared to those recorded from electropherograms gathered under identical conditions. As seen in Table 1, the velocity data obtained from the N Gaussian Model are within 7% of the velocities obtained via electropherograms. This is a remarkable result as the velocity obtained from the N Gaussian Model corresponds to the group velocity of a particular population of DNA molecules, not that of an individual molecule. The proximity of molecular velocities during injection indicates that DNA molecules begin to separate immediately, before they migrate into the separation channel.

Second, the chemical composition of the DNA samples is verified using the area of each Gaussian. The areas underneath the different peaks of the electropherogram illustrate the percentage of the total signal attributed to molecules of different sizes. From our electropherogram data, 21% of the total signal is obtained from DNA molecules less than 150 bases in length, 27% can be attributed to fragments longer than 800 bases, and the remaining 52% is recorded from the fluorescent detection of fragments 150−800 bases in length. Using the areas of each Gaussian in our model, Table 1 also illustrates how the signal distribution mimics

(34) PE Applied Bio Systems, *1998 Automated DNA Sequencing/ABI Prism 310 User's Manual*, Foster City, CA, 1998.
(35) Ogston, A. G. *Trans. Faraday Soc.* **1958**, *54*, 1754−1757.
(36) Slater, G. W.; Guo, H. L. *Electrophoresis* **1996**, *17*, 977−988.
(37) deGennes, P. G. *Scaling Concepts in Polymer Physics*; Cornell Publishers: Ithaca, NY, 1989.
(38) Semenov, A. N.; Rubinstein, M. *Eur. Phys. J. B* **1998**, *1*, 87−94.
(39) Duke, T.; Viovy, J. L.; Semenov, A. N. *Biopolymers* **1994**, *34*, 239−247.
(40) Heller, C. *Electrophoresis* **2001**, *22*, 629−643.

Table 2. Experimentally Measured Values of the Stacking Parameter, P_S, Obtained from the Electrophoretic Injection of Polydisperse Solutions within 250-μm-Long Injectors[a]

	DNA < 150 b		DNA 150−800 b		DNA > 800 b	
V_R (V/cm)	W_F (μm)	P_S (%)	W_F (μm)	P_S (%)	W_F (μm)	P_S (%)
Spin-Column-Purified DNA Samples						
150	86	65.6	184	26.4	240	4.1
200	81	67.6	172	32.2	239	4.4
250	74	70.4	161	35.6	238	4.8
300	68	72.8	150	40.8	237	5.2
350	61	75.6	143	42.8	237	5.2
Ethanol-Precipitated DNA Samples						
150	98	60.8	198	20.8	245	2.0
200	92	63.2	182	27.2	243	2.8
250	83	66.8	175	30.1	243	2.8
300	74	70.4	160	36.0	240	4.1
350	70	72.0	149	40.4	239	4.4

[a] The applied run voltage is represented by V_R, the final width of a Gaussian distribution of DNA molecules is denoted by W_F, and the percentage of stacking exhibited by DNA molecules is illustrated by the parameter, P_S.

these results with values of 18%, 35%, and 47%, respectively. Note, these values also conform to the size-based analysis discussed previously.

Stacking Width and Stacking Parameter. In the above analysis, the Gaussian width of each velocity group is left as a time-evolving parameter. This width can be used to quantify the effect of sample concentration by stacking. Using this approach, we define a stacking parameter, P_S, to represent the percent change in the width of the sample distribution upon electrophoretic injection:

$$P_S = \frac{W_I - W_F}{W_I} \times 100\% \quad (4)$$

where W_I is the width of the initial distribution of DNA molecules prior to electrophoretic injection and W_F is the width of the final DNA distribution when injection is completed. The width of the initial distribution of all molecules, W_I, is well represented by the offset length of the injector because DNA molecules are uniformly distributed within it during sample loading. The final distribution of molecules of interest is then quantitatively determined by using the standard deviation, or width, of the appropriate Gaussian; where the fastest Gaussian is assigned to molecules that migrate via molecular sieving, the intermediate Gaussian represents molecules that travel via reptation and the slowest Gaussian represents the migration of the longest molecules in the sample.

During an electrophoretic injection at 150 V/cm, using samples purified via spin columns and a 250-μm-long injector, the distribution of the smallest DNA fragments resembled a Gaussian profile whose width was less than 20% of the width of the original sample plug, i.e., $W_F = 0.2W_I$. Similarly, molecules within the intermediate Gaussian were concentrated to generate a sample plug whose width was less than 35% of the original sample. Closer inspection of the data shown in Table 2 illustrates the Gaussian distributions of all molecules become increasingly narrow under larger applied voltage. Further, smaller DNA molecules are always more tightly stacked than medium- and larger-sized molecules regardless of the experimental conditions imposed.

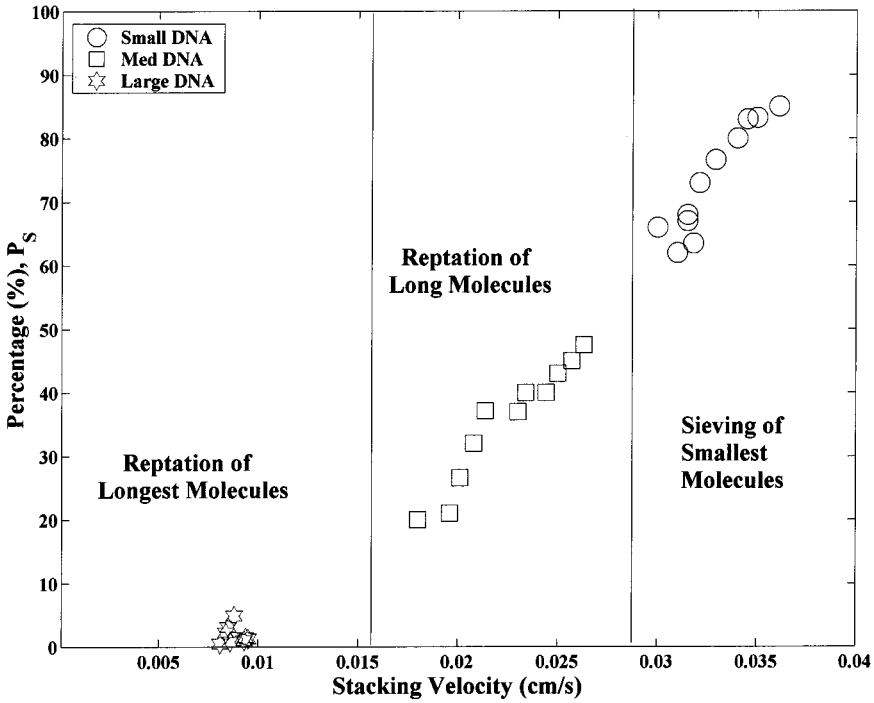

Figure 4. Analytically obtained values of the stacking velocity, V_{ST}, plotted against the experimental measurements of the newly defined stacking parameter, P_S. The graph incorporates data compiled from experiments using devices with 3 independent injector lengths, 2 separate sample purification methods, and 10 different values of applied voltage. Circular markers represent the measurements of smaller DNA molecules (less than 100 bases in length), and measurements of medium-sized (100−850 bases) and larger DNA molecules (greater than 850 bases in length) are illustrated by square and star-shaped markers, respectively.

Empirical Tool for Stacking Estimates. Ideally, we wish to incorporate all experimental parameters of interest into one value that can be used to estimate the level of stacking produced. The analytical expression for the stacking velocity, V_{ST}, discussed in the Moving Boundary Equation section, is an ideal candidate in this regard because it incorporates injector length, conductivity, DNA size, and run voltage. As a result, experimental measurements of the stacking parameter, P_S, are plotted against the analytical values of stacking velocity, V_{ST}, in Figure 4. The data illustrate that smaller DNA molecules will always become more concentrated during injection than larger-sized molecules. As seen, levels of the stacking parameter, P_S, are consistently highest within the population of smallest molecules. Figure 4 also illustrates that few combinations of experimental parameters can induce any significant level of stacking within the population of longest molecules. As seen, the stacking dynamics of each population of molecules remain distinct. The data in Figure 4 indicate that smaller DNA molecules will always stack more readily than medium- or longer-sized molecules regardless of the injector, sample purification, or applied voltages used. Figure 4 also illustrates that few combinations of experimental parameters can induce any significant level of stacking within the population of longest molecules. By representing the stacking behavior of DNA molecules in this manner, it is possible to use Figure 4 to modify electrophoretic parameters or redesign microdevice geometry to achieve better stacking for molecules of interest.[22]

High-Voltage Injection Protocol. It is experimentally desirable to optimize electrophoretic injection because increased sample concentration via stacking has consistently produced separations of higher resolution and quality. Unfortunately, the combinations of parameters used in Figure 4 only increase the concentration of molecules of particular molecular weights, not the overall level of stacking experienced by the entire sample. Hence, a new high-voltage injection protocol has been developed to increase the overall level of stacking experienced by all molecules within the sample.

Although numerous researchers[2,11,28] have documented the negative effects of high run voltages, V_R, during separation, our newest experiments indicate that short periods of high voltage during injection do not destroy the quality of DNA separations. We have designed a new high-voltage injection protocol that utilizes ultrahigh voltages during injection only, to increase the sample concentration effect during stacking. Whereas conventional separations utilize two distinct voltages, the load voltage, V_L, during sample loading, and the run voltage, V_R, during injection and separation, our protocol uses three: the load voltage, V_L, an injection voltage, V_I, and the run voltage, V_R. DNA molecules are still loaded into the sample using V_L, but now, a distinct injection voltage, V_I, is used to introduce DNA molecules into the separation channel. Values of V_I can be significantly greater than V_R but are only applied for a maximum of 5 s. After this, the voltage is instantaneously reduced to the standard run voltage, V_R, for the remainder of the separation.

Figure 5 demonstrates the shape of the stacked sample at the exit of a 250-μm-long cross-injector offset after electrophoretic injection was performed using six different values of injection voltage, V_I. The set of six images on the left-hand side displays the digital image of the sample plug obtained through video microscopy. The corresponding set of images on the right-hand side display the fluorescence intensity of each molecular distribution within the sample plug as measured along the channel centerline. Images are arranged in order of increasing injection voltage as indicated by the values of V_I on the upper-left-hand corner ranging from $V_I = 236$ V/cm to $V_I = 708$ V/cm. The digital images represent the molecular redistribution of the sample when electrophoretic injection is complete. As seen, the distribution and overall width of the sample plug decrease quickly with increasing voltage.

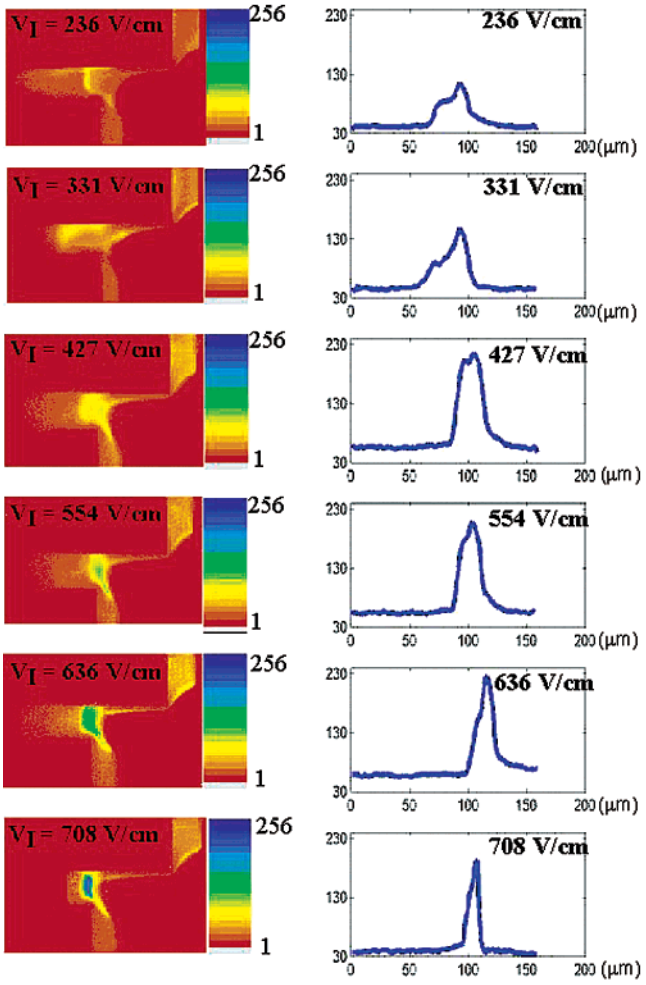

Figure 5. Set of six digital images on the left-hand side representing the shape of the 10^{-10} M polydisperse sample at the end of electrophoretic injection, as captured in real time via video microscopy. In each image, the sample arm of the cross-injector is seen on the upper-right-hand side while the waste arm is shown on the lower left. The cathode and anode are located at the far right and left, respectively, of the main separation channel oriented horizontally in each image. Each image illustrates the stacked sample plug generated via the high-voltage injection protocol described here. All experiments utilized a load voltage, V_L, of 300 V/cm and run voltage, V_R, equal to 150 V/cm. The different values of injection voltage, V_I, used for each experiment are shown in the upper-left-hand corner of the images. The set of six graphs on the right-hand side of the figure illustrates the corresponding intensity profile of each stacked sample plug.

The first image taken using an injection voltage of $V_I = 236$ V/cm represents the conditions derived using run voltages only slightly higher than conventional values of V_R. As seen, the width of the sample plug is fairly wide and its molecules exhibit three

Table 3. Width of the Stacked DNA Sample during Electrophoretic Injection Using High-Voltage Protocols[a]

V_I (V/cm)	W_F (μm)	W_{fwhm} (μm)
236	73	
394	62	
426	55	21
554	51	19
630	40	15
708	27	9

[a] Widths of the sample, W_F, were experimentally determined via microscopy measurements taken at the channel centerline. Further numerical analysis of intensity measurements provided an additional full width at half-maximum representation, W_{fwhm}, where applicable. Sample loading was performed for a 3-min period at 300 V/cm prior to all injection experiments.

Table 4. Read Lengths and Resolution Measurements, R_L, Obtained from Separations Performing High-Voltage Injection Protocols[a]

V_I (V/cm)	read lengths (bases)	highest R_L (bases)	average R_L
236	50−510	150−250	0.42
554	52−512	178−310	0.55
708	55−510	250−325	0.57

[a] All separations were performed using spin-column-purified 10^{-10} M sequencing reactions, 2% solutions of 9-MDa LPA, a load voltage of $V_L = 300$ V/cm, and a run voltage of $V_R = 150$ V/cm within identical 250-μm-length injectors. Actual electrophoretic injections were performed at the elevated injection voltages, V_I, denoted on the table.

visually distinguishable regions of DNA as discussed under Intensity Profiles. Using $V_I = 394$ V/cm, the width of the sample plug is slightly decreased and its distribution of DNA is significantly more compact. The electrophoretic injection performed using $V_I = 473$ V/cm is the first to illustrate the improved stacking dynamics desired. Here, 92% of the stacked sample area is represented by one Gaussian distribution, while only traces of DNA molecules are unstacked. The stacked samples developed using injection voltages of 552, 630, and 709 V/cm demonstrate decreasing widths and increasingly concentrated sample plugs. From the data illustrated in Figure 5, the distribution of all DNA molecules is near perfectly Gaussian when electrophoretic injection is performed using $V_I > 630$ V/cm. The width of each stacked sample is shown in Table 3.

As done previously in the Correlation with DNA Sequencing Results section, the microscopy results within the injector are correlated to the data obtained from electropherograms. Table 4 displays the results of the separations performed under the identical experimental conditions discussed. As shown, the separations indicated a 35% increase in resolution and 25% increase in DNA read length for molecules 150−300 bases in length. These preliminary experiments indicate that higher levels of stacking may be the key to obtaining increased read lengths during separations. Although the optimal benefits of stacking will surely depend on a detailed match of the channel geometry and experimental conditions with the desired assay, the modified high-voltage protocol will certainly assist in this effort.

CONCLUSIONS

In this study, digital imaging was used to explore the electrophoretic injection of various populations of DNA molecules within microfabricated injectors. The distinct migration of molecules during sample loading was well illustrated by the images, as was the complexity of DNA redistribution during the stacking process. Data analyzed using the *N* Gaussian model were decomposed into different velocity groups during injection. This analysis illustrated the formation of three distinct DNA populations sorted according to mobility. The intensity profiles gathered via digital imaging further demonstrated the increased level of stacking induced by high-voltage injections. These effects resulted in increased read lengths and higher resolution measurements. Using the synergy of digital images taken within the cross-injector and electropherograms detected within the separation channel, we have used a "total analysis" approach that will lead to improvements and increased applicability of microdevice separations.

ACKNOWLEDGMENT

The authors thank Mark Novotny and Lance Koutny for their contributions to this publication, as well as Nicki Watson, for her microscopy expertise, and Tom O'Neil, for his guidance in device manufacture. This work was supported by the National Institute of Health (NIH), the National Institute of Justice (NIJ), Air Force Office of Science Research (AFOSR), and the Defense Advanced Research Projects Agency (DARPA).

Received for review September 17, 2001. Accepted February 4, 2002.

AC0110045